ELECTRONICS AND ELECTRICAL ENGINEERING
ISSN 1392 – 1215 2011. No. 1(107)
ELEKTRONIKA IR ELEKTROTECHNIKA

HIGH FREQUENCY TECHNOLOGY, MICROWAVES
T 191
AUKŠTŲJŲ DAŽNIŲ TECHNOLOGIJA, MIKROBANGOS

Investigation of the Electromagnetic Fields in Gyrotropic Waveguides

V. Mališauskas, T. Sledevič
Department of Electronic Systems, Vilnius Gediminas Technical University, Naugarduko str. 41-424, LT-03227 Vilnius, Lithuania, phone: +370 672 04450, e-mail: vacius.malisauskas@el.vgtu.lt

Introduction

Open cylindrical round cross-section gyrotropic waveguides (GW) manufactured using semiconductor, ferrite and dielectric are broadly used in the electromagnetic (EM) microwave devices. Their design is convenient for production and they have a wide working frequency band [1–3]. However structures of their EM fields are not completely investigated. This limits application of the GW.

In this paper a methodology for the digital and visual investigation of the EM fields in GW is developed using a mathematical model [1] of waveguides.

The solutions of transcendental dispersion equations are needed to calculate strength of the EM fields components in GW. These solutions are inserted into equations of the components, next, distribution functions of EM fields strength [1] are calculated, and then the EM fields in two-dimensional and three-dimensional spaces are visualized.

General electrodynamical and mathematical models of gyrotropic waveguides

Basic electrodynamical model of the open cylindrical round cross-section GW in cylindrical coordinate r, φ, z system is presented in Fig. 1 [1–5].

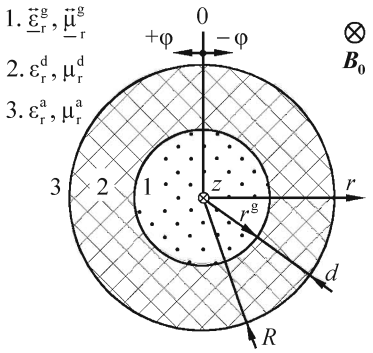

Fig. 1. Basic electrodynamical model of the open cylindrical round cross-section GW: 1 – semiconductor, ferrite or dielectric core; 2 – external non-magnetic dielectric layer; 3 – air

This model is suitable for large class of gyrotropic and dielectric waveguides. It estimates the gyrotropic, artificially induced in ferrite and semiconductor waveguides by the external constant longitudinal magnetic field which flux density vector is $\boldsymbol{B}_0$.

Model area 1 (Fig. 1) is a semiconductor, ferrite or dielectric core. It is characterized by complex permittivity and permeability tensors $\underline{\ddot{\varepsilon}}_r^g, \underline{\ddot{\mu}}_r^g$ and real permeability and permittivity μ_r^g, ε_r^g respectively. Model area 2 is an external non-magnetic dielectric layer with the real relative permittivity ε_r^d and permeability $\mu_r^d = 1$. Model area 3 is air with real relative permittivity and permeability $\varepsilon_r^a = \mu_r^a = 1$.

The part of basic mathematical GW model [1] is presented below.

The wave type of the GW is defined by distribution of longitudinal components of EM fields in the waveguide cross-section. The complex of longitudinal electric field strength in model's area 1 (Fig. 1) is described by equation

$$\underline{E}_z^g(\underline{k}_{\perp 1,2}^g r, \varphi, z, t, m) = \left[\underline{a}\underline{A}_1 \mathrm{J}_m(\underline{k}_{\perp 1}^g r) + \right.$$
$$\left. + \underline{B}_1 \mathrm{J}_m(\underline{k}_{\perp 2}^g r)\right] \mathrm{e}^{\pm \mathrm{i} m\varphi}\, \mathrm{e}^{-\mathrm{i}\underline{h}z}\, \mathrm{e}^{\mathrm{i}\omega t}, \quad (1)$$

where $\underline{a}$ is waves coupling coefficient, which indicates the proportion mixes E and H type waves in hybrid modes; $\underline{A}_1, \underline{B}_1$ – unknown amplitude coefficients; $\mathrm{J}_m(\underline{k}_{\perp 1,2}^g r)$ is the Bessel cylindrical function of the first kind m-th order; $\underline{k}_{\perp 1,2}^g r$ – first and second internal transverse waves numbers normalized to radius r; $m = 0, 1, 2, \ldots$ are waves azimuthal periodicity index; $\pm\varphi$ – the azimuth angles of the left and right polarized waves; $\mathrm{e}^{-\mathrm{i}\underline{h}z}$ – the EM waves dependence on z; $\underline{h} = h' - \mathrm{i}h''$ is the longitudinal waves number, where h' – EM waves phase coefficient, h'' is the damping coefficient; $\mathrm{e}^{\mathrm{i}\omega t}$ is the dependence on fields angular frequency ω and time t.

EM fields distribution in waveguides doesn't depend on the damping coefficient h'', so imaginary values aren't included in the calculations. Function $e^{\pm i m\varphi}$ is writing under the Euler equation and real part is taken only. Additionally it's considered that $z=0$, $t=0$, $\underline{A}_1 = \underline{B}_1 = 1$, $a = Re(\underline{a})$. In this manner distribution functions of the EM fields strength longitudinal components only under gyrotropic waveguides coordinate r and φ are derived.

Then, the longitudinal electric field strength in gyrotropic core distribute according to function, derived from the equation (1)

$$E_z^{\mathrm{g}}(k_{\perp 1,2}^{\mathrm{g}} r, \varphi, m) = \left[a\,\mathrm{J}_m(k_{\perp 1}^{\mathrm{g}} r) + \mathrm{J}_m(k_{\perp 2}^{\mathrm{g}} r) \right] \cos(m\varphi). \quad (2)$$

The distribution function of the longitudinal electric field strength in model area 2 is described as follows

$$E_z^{\mathrm{d}}(k_{\perp}^{\mathrm{d}} r, \varphi, m) = \left[\mathrm{J}_m(k_{\perp}^{\mathrm{d}} r) + \mathrm{N}_m(k_{\perp}^{\mathrm{d}} r) \right] \cos(m\varphi), \quad (3)$$

where $\mathrm{J}_m(k_{\perp}^{\mathrm{d}} r)$ is the first kind Bessel and m-th order Neumann cylindrical functions with argument $k_{\perp}^{\mathrm{d}} r$. It's internal normalized transverse wave's number in the dielectric.

The distribution function of the longitudinal electric field strength in model area 3 is described by equation

$$E_z^{\mathrm{a}}(k_{\perp}^{\mathrm{a}} r, \varphi, m) = \mathrm{H}_m^{(2)}(k_{\perp}^{\mathrm{a}} r) \cos(m\varphi), \quad (4)$$

where $\mathrm{H}_m^{(2)}(k_{\perp}^{\mathrm{a}} r)$ is the second kind cylindrical Hankel function with argument $k_{\perp}^{\mathrm{a}} r$, it's external normalized transverse waves number in air.

The distribution functions of the longitudinal magnetic field strength are derived by analogy. The transverse components are calculated from the equations of longitudinal components using Hamilton operator ∇.

General algorithm to calculate the EM fields strength distribution

In this paper general algorithm to calculate the EM fields strength distribution is created (Fig. 2).

Following steps of the algorithm may be noted.

1. Input of the solutions $h'r^{\mathrm{g}}(fr^{\mathrm{g}})$ of transcendental dispersion equations and other parameters [1].
2. Calculation of electrodynamical coefficients.
3. Calculation of special Bessel, Neumann and Hankel cylindrical functions.
4. Calculation of the EM fields longitudinal (2–4) and transverse components [1].
5. Check of boundary conditions for electric $E_z^{\mathrm{g}}(r^{\mathrm{g}}) = E_z^{\mathrm{d}}(r^{\mathrm{g}})$, $E_z^{\mathrm{d}}(R) = E_z^{\mathrm{a}}(R)$ and magnetic $H_z^{\mathrm{g}}(r^{\mathrm{g}}) = H_z^{\mathrm{d}}(r^{\mathrm{g}})$, $H_z^{\mathrm{d}}(R) = H_z^{\mathrm{a}}(R)$ fields, where r^{g} is boundary between area 1 and 2 of waveguide model; R is boundary between area 2 and 3.
6. Selection of transverse 2D or longitudinal 3D section. Selection of the EM fields strength imaging method. It may be: vectors lines, colour contours or areas of equal strength.
7. Imaging of the EM fields strength distribution. Output of tables and graphs.

The distribution of the EM fields strength longitudinal components in GW is calculated by using our proposed general algorithm and our created program in *MATLAB®*.

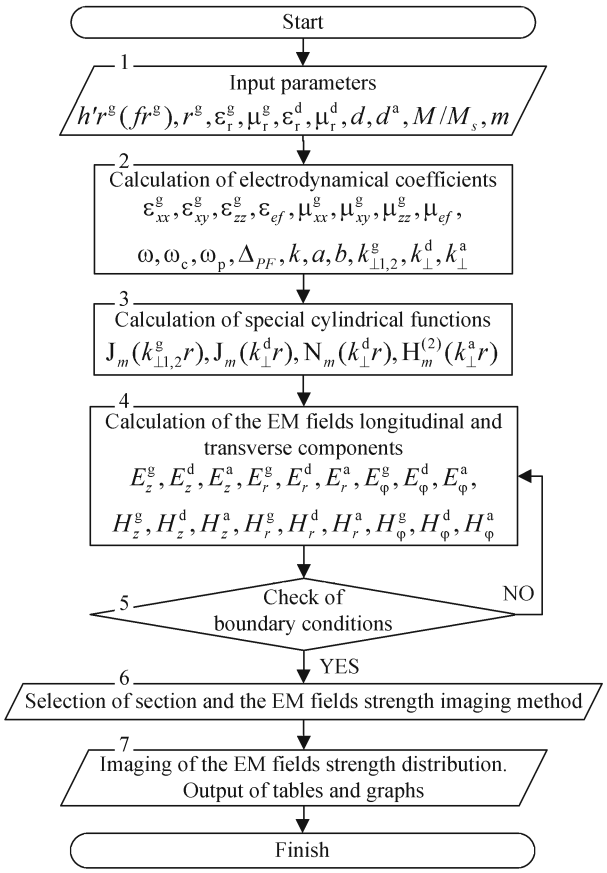

Fig. 2. General algorithm to calculate the EM fields strength distribution

The EM fields strength distribution is presented below using contours of equal strength, though it may be presented as strength vectors lines, as it shown in [5].

Investigation of the EM fields distribution in dielectric waveguides

To test our proposed algorithm and written program, the EM fields distribution is investigated in dielectric waveguides. Relative dielectric permittivity of the core material TM15 is $\varepsilon_{\mathrm{r}}^{\mathrm{d}} = 15$, its radius $r^{\mathrm{d}} = 1$ mm. The waveguide is surrounded by air which thickness $d^{\mathrm{a}} = 1.5$ mm.

In Fig. 3 (*a*–*d*) distribution the EM fields at $m = 0$, when normalized frequency $fr^{\mathrm{d}} = 0.04$ GHz·m, is presented. Bold dots in Fig. 3–6 mark the areas, where EM fields strength lines are aimed at us, crosses – from us. In Figs. 3 (*c*, *d*) and 4 (*c*, *d*) the letter r (red) mark the areas, where strength of EM fields is the maximal positive, b (blue) – maximal negative, g (green) – close to zero.

It is seen in Figs. 3 (*a*) and (*c*) that electric field hasn't longitudinal components in the dielectric

waveguide. The strongest magnetic field is in the centre of dielectric core (Fig. 3 (*b, d*)) and much weaker in the opposite direction is in external air layer near the boundary with the dielectric. This EM fields distribution is characterized by mode H_{01}. The separate modes H and E with azimuthal periodicity index $m = 0$ (H_{01}, E_{01}, H_{02}, E_{02}, ...) may exist in dielectric waveguides [1].

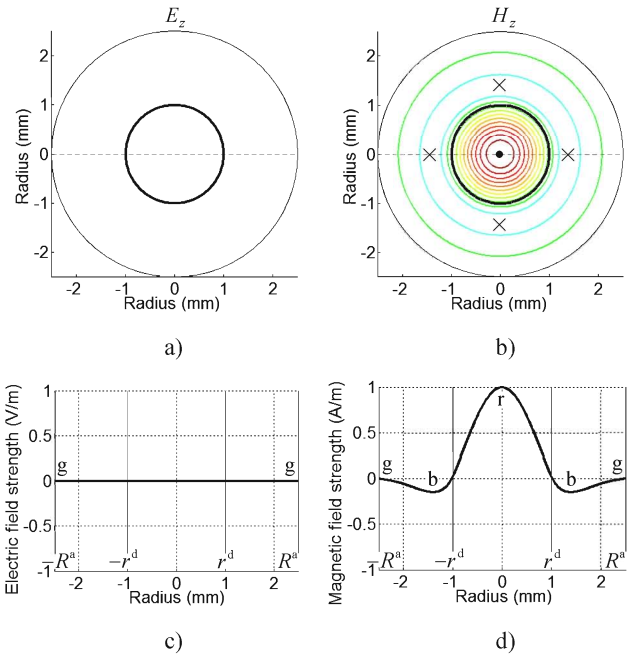

Fig. 3. Distribution of EM fields of mode H_{01} in dielectric waveguides cross-section (*a*, *b*) and in horizontal plane (*c*, *d*)

In Fig. 4 (*a–d*) distribution of EM fields in the cross-section of earlier specified dielectric waveguide, at $m = 1$, and normalized frequency $fr^d = 0.05$ GHz·m is presented.

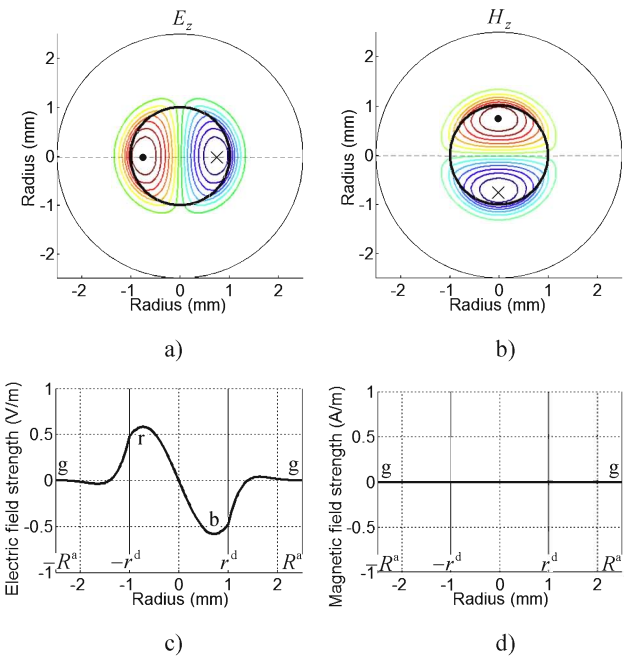

Fig. 4. Distribution of EM fields of mode HE_{11} in dielectric waveguides cross-section (*a, b*) and in horizontal plane (*c*, *d*)

In Fig. 4 (*a*) the electric field is rotated at 90° in respect of magnetic field in Fig. 4 (*b*). The electric field is the strongest and magnetic is equal to zero in the horizontal plane shown by dashed line. It is seen that fields are symmetric by the horizontal and vertical. This feature is typical to all the waves in space and time in all waveguides [1]. Therefore, this investigation can rely on.

Distribution functions of the longitudinal electric and magnetic fields are similar and include 2 sharp extremes in dielectric waveguides near the boundary with the air layer. Moreover, there are 2 mild extremes in surface air layer.

This EM fields distribution is characterized by hybrid mode HE_{11}.

Investigation of the EM fields distribution in GW

The longitudinal EM fields are investigated in semiconductor and semiconductor-dielectric *n*-InSb waveguides. They are exposed to constant longitudinal magnetic field which flux density $B_0 = 1$ T. Dielectric constant of semiconductor grating is $\varepsilon_k^{sn} = 17.7$, and electron concentration $N = 5 \cdot 10^{19}$ m^{-3}. Semiconductor core's radius is $r^s = 1$ mm. Without the external dielectric layer, the core is surrounded by air which thickness $d^a = 1.5$ mm. The external dielectric layer's, when it is, thickness $d = 0.5$ mm. Its relative dielectric permittivity is $\varepsilon_r^d = 15$. In this case, dielectric is surrounded by air which thickness $d^a = 1$ mm.

In Fig. 5 (*a, b*) distribution of EM fields of main mode HE_{11} in semiconductor *n*-InSb waveguides at normalized frequency $fr^s = 0.025$ GHz·m is presented. The longitudinal EM fields are concentrated in semiconductor core near the boundary with the air layer.

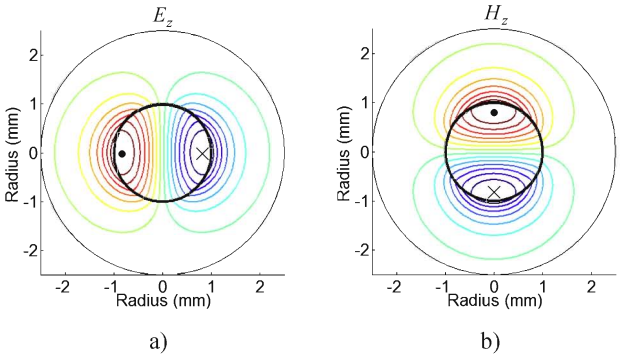

Fig. 5. Distribution of EM fields of mode HE_{11} in the cross-section of the semiconductor waveguide at $fr^s = 0.025$ GHz·m

In Fig. 6 (*a, b*) distribution of EM fields strength of main mode HE_{11} in the earlier specified semiconductor *n*-InSb waveguides at normalized frequency $fr^s = 0.05$ GHz·m is presented. It is seen that the longitudinal EM fields are concentrated in the semiconductor core more than in the dielectric core shown in Figs. 4 (*a*) and (*b*). This is explained by the higher than $\varepsilon_r^d = 15$ semiconductor background dielectric constant $\varepsilon_k^{sn} = 17.7$ and by the much larger concentration of free electrons.

Let we compare Fig. 5 (*a*, *b*) and Fig. 6 (*a*, *b*). It is evidence, that at lower frequency, a large part of EM wave is transmitted by air (Fig. 5 (*a*, *b*)). By doubled frequency the extremes of the EM fields strength retreat to the middle of waveguide and the fields are almost entirely concentrated in the core (Fig. 6 (*a*, *b*)). So, the surface layer of high frequency EM waves becomes tightened.

In Fig. 6 (*c*, *d*) distribution of EM fields strength of mode HE_{11} in semiconductor-dielectric *n*-InSb waveguides is presented. It's seen here that external dielectric layer pull up the longitudinal EM fields from the semiconductor core into dielectric and air. The EM fields here have 4 fairly sharp extremes of strength at semiconductor core boundary with the dielectric layer and in the external air layer. This distribution of EM fields doesn't present in any literature.

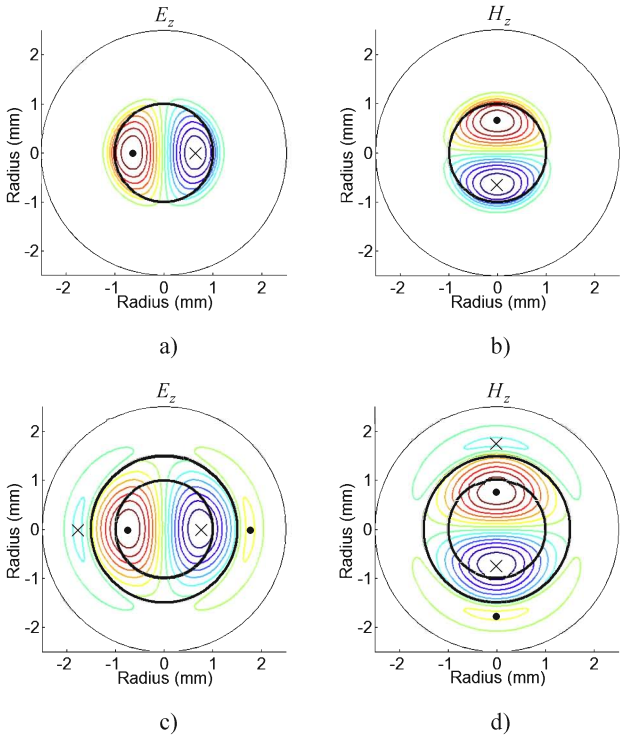

Fig. 6. Distribution of EM fields of mode HE_{11} in semiconductor (*a*, *b*) and semiconductor-dielectric (*c*, *d*) *n*-InSb waveguides at $fr^{s} = 0.05\ \text{GHz} \cdot \text{m}$

Conclusions

General algorithm, program in *MATLAB*® and technique for investigation of the distribution of the electric and magnetic fields in open cylindrical round cross-section GW are developed. The program is tested for modes H_{01}, HE_{11} in dielectric waveguides on TM15 dielectric type. Testing showed that the investigation can rely on.

The EM fields distribution of the mode HE_{11} is investigated in gyroelectric semiconductor and semiconductor-dielectric *n*-InSb waveguides.

The EM fields distribution images are consistent with physical nature of the fields in all waveguides. It also confirms the correctness of calculated distribution of EM fields in gyrotropic waveguides.

The EM fields are concentrated in cores of gyrotropic waveguides when normalized frequency is increased.

The external dielectric layer changes the EM fields distribution in gyrotropic waveguides. In this case the EM fields are partly redistributed from gyrotropic cores to dielectric layer and the air.

References

1. **Nickelson L., Ašmontas S., Mališauskas V., Šugurovas V.** Open Cylindrical Gyrotropic Waveguides. – Monograph. – Vilnius: Technika, 2007. – 248 p. (in Lithuanian).
2. **Liu S., Li L. W., Leong M. S., Yeo T. S.** Theory of Gyroelectric Waveguides // Progress in Electromagnetics Research (PIER 29), 2000. – P. 231–259.
3. **Hogenboom D., Oliver S., DiMarzio C.** Light Propagation in a Planar Dielectric Waveguide with a Gyrotropic Layer // Applied Optics. – Massachusetts: Optical Society of America, 1998. – No. 31(37). – P. 7218–7222.
4. **Al–Gawagzeh M. Y.** The Effect of Dielectric Permeability in Anisotropic Bending Spiral Optical Fiber on Transmission Parameters // Electronics and Electrical Engineering. – Kaunas: Technologija, 2009 – No. 1(89). – P. 45–48.
5. **Nickelson L., Gric T., Asmontas S., Martavičius R.** Electric Field Distributions of the Fast and Slow Modes Propagated in the Open Rod SiC Waveguide // Electronics and Electrical Engineering. – Kaunas: Technologija, 2009. – No. 5(93). – P. 87–90.

Received 2010 10 01

V. Mališauskas, T. Sledevič. Investigation of the Electromagnetic Fields in Gyrotropic Waveguides // Electronics and Electrical Engineering. – Kaunas: Technologija, 2011. – No. 1(107). – P. 29–32.

In this paper a general algorithm, program in *MATLAB*® environment and technique to investigate electromagnetic (EM) fields in gyrotropic waveguides are created. To test them distribution of EM fields of modes H_{01}, HE_{11} were investigated in dielectric waveguides. Distribution of EM fields of mode HE_{11} in gyroelectric semiconductor and semiconductor-dielectric *n*-InSb waveguides are investigated. Dependence of distribution of EM fields of the hybrid main mode HE_{11} in semiconductor *n*-InSb waveguides on normalized frequency and external dielectric layer is defined. Ill. 6, bibl. 5 (in English; abstracts in English and Lithuanian).

V. Mališauskas, T. Sledevič. Elektromagnetinių laukų girotropiniuose bangolaidžiuose tyrimas // Elektronika ir elektrotechnika. – Kaunas: Technologija, 2011. – Nr. 1(107). – P. 29–32.

Šiame darbe sukurti bendrieji algoritmas, programa *MATLAB*® terpėje ir metodika elektromagnetiniams (EM) laukams girotropiniuose bangolaidžiuose tirti. Jų patikrai ištirtas H_{01}, HE_{11} bangų EM laukų pasiskirstymas dielektriniuose bangolaidžiuose. Ištirtas HE_{11} bangos EM laukų pasiskirstymas giroelektriniuose puslaidininkiniuose ir puslaidininkiniuose-dielektriniuose bangolaidžiuose iš *n*-InSb puslaidininkio. Nustatyta hibridinės HE_{11} pagrindinio tipo bangos EM laukų pasiskirstymo priklausomybė nuo normuotojo dažnio ir išorinio dielektriko sluoksnio puslaidininkiniuose *n*-InSb bangolaidžiuose. Il. 6, bibl. 5 (anglų kalba; santraukos anglų ir lietuvių k.).

DOI: 10.5755/j02.eie.9077